Review

For reprint orders, please contact: reprints@futuremedicine.com

Biomarkers in Medicine

Can nanotechnology improve cancer diagnosis through miRNA detection?

miRNAs are key regulators of gene expression, and alterations in their expression levels correlate with the onset and progression of cancer. Although miRNAs have been proposed as biomarkers for cancer diagnosis, their application in routine clinical praxis is yet to come. Current quantification strategies have limitation, and there is a great interest in developing innovative ones. Since a few years, nanotechnology-based approaches for miRNA quantification are emerging at fast pace but there is urgent need to go beyond the proof-of-concept stage. Nanotechnology will have a strong impact on cancer diagnosis through miRNA detection only if it is demonstrated that the newly developed approaches are indeed working on 'real-world' samples under standardized conditions.

First draft submitted: 18 July 2016; Accepted for publication: 24 October 2016; Published online: 5 December 2016

Keywords: miRNA • nanoparticles • nanotechnology • oncology • sensors

Roberto Fiammengo
Center for Biomolecular Nanotechnologies@UniLe – Istituto Italiano di Tecnologia (IIT), Via Barsanti, 73010 Arnesano, Lecce, Italy
*Author for correspondence: roberto.fiammengo@iit.it

miRNA detection & quantification for cancer diagnosis

miRNAs constitute the major class of endogenous small noncoding RNAs found in all living organisms and play a fundamental role as regulators of gene expression. Mature miRNAs are single-stranded oligoribonucleotides with a typical length between 18 and 25 nucleotides. The mechanisms by which miRNAs regulate gene expression have been investigated in many studies and extensively reviewed [1–4]. Each miRNA can regulate the expression of hundreds of genes, simultaneously affecting multiple cellular pathways. Furthermore, each mRNA can be target of many different miRNAs [5]. Under pathological conditions such as in cancer, dysregulated miRNA levels are observed [6]. However, the relationship between dysregulated miRNA levels and cancer is not straightforward. In particular, each type of cancer is characterized by alterations in the expression of a more or less broad panel of miRNAs [7–9]. Thus, miRNA profiling in combination with current standardized diagnostic tools such as histopathological diagnosis is fundamental for the identification of the minimal, representative miRNA panel allowing secure cancer diagnosis. In general, alteration of the expression level of a single miRNA has not sufficient diagnostic power and therefore any miRNA detection strategy should be amenable to multiplexing, in other words, the parallel detection/quantification of known multiple miRNAs.

Another important aspect of using miRNAs as biomarkers for cancer diagnosis concerns the identification and validation of the most promising specimen source among tissue biopsies, blood, plasma or serum and other body fluids. Following the discovery of circulating miRNAs [10,11], there has been an enormous interest in identifying and validating panels of circulating miRNAs related to the onset and progression of cancer. Circulating miRNAs are stable and protected from RNAse activity and may allow using a simple blood sample for cancer diagnosis in

Future Medicine part of fsg

place of a more invasive biopsy [12–15]. Other body fluids such as saliva, urine, seminal fluid, cerebrospinal fluid, breast milk and even tears contain measurable amounts of extracellular miRNAs [16]. However, a recent critical evaluation of the literature in this field suggests that circulating miRNAs are still far away from becoming actual biomarkers of practical clinical utility [17]. Indeed, most of the problems seem to be related to a widespread lack of reproducibility among studies dealing with miRNA profiling and are not exclusive to circulating miRNAs. Specimens of different origin have largely different miRNA content (Table 1) [16], differently biased composition (cellular vs extracellular) and require different preparative steps prior to miRNA quantification, with the possibility of introducing additional bias during sample preparation. One major cause of irreproducibility between different studies is thus related to sample processing, which includes specimen collection and storage, isolation of total RNA and separation/enrichment of the small RNA fraction when necessary [16,18–20]. A second relevant cause of irreproducibility relates to the lack of universally accepted and validated internal references for miRNA quantification [21,22]. This lack of consensus in the selection of internal standards has a profound effect on the observed miRNA levels determined in different studies with different technological platforms [23–25].

Challenges faced by miRNA quantification methods

Current conventional methods for miRNA detection and quantification are: northern blotting, quantitative reverse transcription (qRT)-PCR, microarrays and next-generation sequencing (NGS). It is beyond the scope of this work to go into the details of each method and the interested reader is referred to two excellent and up-to-date review articles [32,33]. Additionally, bead-based technologies, such as Luminex's xMAP® (TX, USA) [34] or the Firefly® particles from Firefly BioWorks (MA, USA) [35], as well as the nCounter® system from NanoString Technologies (WA, USA) [36] are possible alternatives for miRNA profiling. These hybridization-based technologies with good multiplexing capability (analogous to microarrays) have appeared on the market in the past few years. Only a few studies have explicitly compared their performances with those of the more widespread approaches mentioned at the beginning of this section [23,37–39].

Here, we would like to stress some general concepts which should be kept in mind when dealing with miRNA quantification for diagnostic purposes. In particular:

- miRNAs constitute only a minute fraction of the total RNA in biological specimens;
- Concentrations of miRNAs may span several orders of magnitude;
- miRNA sequences may differ just in one to a few nucleotides;
- Extracted RNA samples may contain variable amounts of pri- and pre-miRNA, the precursors of mature miRNA, potentially affecting quantification;
- Mature miRNAs are often present as iso-miRs, sequences with varying termini due to variations in precursor processing by Drosha and/or Dicer enzymes;
- A wide range of melting temperatures (T_m) is observed for duplexes composed of miRNAs and nucleic acid probes.

These peculiar features of miRNA, pose burdens and limitations to any quantification strategy. An overview of the main advantages and limitations of the established miRNA quantification methods is provided in Table 2 with the aim of supporting the reader in understanding the drive to develop new strategies [40,41]. In the following sections of this review, we will critically analyze the contribution of nanotechnology to this field in the past 2 years. Several innovative approaches based on the special properties of nanostructured materials and devices have appeared in the scientific literature [42] and are expected to support the widespread adoption of miRNA biomarkers for cancer diagnosis. One important contribution of nanotechnology to the detection of miRNAs could come from the development of point-of-care testing, as demonstrated by the recent developments in other field of clinical diagnostics [43].

Nanotechnology-based methods for miRNA quantification

Detection and quantification of miRNAs are based on a molecular recognition event, typically the hybridization of a miRNA strand with a nucleic acid probe (or a synthetic analog) via Watson–Crick base pairing, which is coupled to a transduction mechanism resulting in a measurable signal. The main difference between nanotechnology-based and conventional methods lies in the transduction mechanism, whereby the peculiar physicochemical properties of nanostructured materials are essential to enhance signal readout. For the purpose of this review, we have grouped nanotechnology-based strategies into three main groups: methods in solution involving nanoparticulate materials, approaches based on nanostructured surfaces and approaches based on the combination of nanoparticulate materials with solid supports.

Table 1. Estimated ranges of miRNA concentration.

Specimen	Sample size	Total RNA (μg)	Amount of each mature miRNA	Expected conc. of each mature miRNA[†]
Cell cultures	10^5 cells	0.2–3.0[‡]	0.3 amol to 30 fmol[§]	3 fM to 3 nM
Tissues	50–100 mg	>5	0.3 amol to 30 fmol[¶]	3 fM to 3 nM
Serum-plasma	200–400 μl	0.05–1[#]	7 zmol to 3 amol[††]	70 aM to 300 fM
Other body fluids	200–400 μl	0.027–14[‡‡]	–	–

miRNA concentrations in an assay mixture may vary over several orders of magnitudes for two main reasons: first, largely variable natural expression levels and second, the combination of specimen origin and sample preparation protocol. More in detail, specimens of different origin present very different miRNA content, and tissue (or cellular) specificity is observed for some miRNAs. Furthermore, the sample preparation protocol may cause miRNA enrichment/concentration or dilution. However, for a selected specimen origin and sample processing procedure, the dynamic range of miRNA concentration is definitely narrower and most probably ≤10^4-fold.
[†]Values calculated assuming assay volumes to be within the 10–100 μl interval (however in some cases larger volumes may be needed).
[‡]The amount of total RNA/cell is estimated between 2 and 30 pg depending on cell type.
[§]The average number of miRNA copies/cell is assumed to vary between 20 and 200,000 depending on the specific miRNA [26–28], accounting for both normal and pathological conditions.
[¶]Assuming a sample size between 0.3 and 3 μg total RNA and miRNA copies/30 pg total RNA varying between 20 and 200,000 depending on the specific miRNA and the specific tissue [29].
[#]Variability depends on the isolation protocol [30].
[††]Estimated from the miRNA copy number per μl serum for five different miRNAs quantified in the sera of breast cancer patients and healthy individuals [31]. Data calculated for 200 μl serum.
[‡‡]Investigated fluids are breast milk, colostrum, saliva, seminal fluid, tears, urine, amniotic fluid, cerebrospinal fluid, plasma, pleural fluid, peritoneal fluid and bronchial lavage [16]. The lowest amount of total RNA was found in urine while the highest corresponds to breast milk. Data are calculated for 300 μl fluid.

Strategies based on nanoparticulate materials

Several nanoparticulate materials (nanoparticles [NPs]) have excellent optical properties making them ideally suited for the development of sensing strategies. Some NPs are bright and stable fluorescence emitters, for example, silver nanoclusters (AgNCs) and quantum dots (QDs), and can be used either directly or in fluorescence resonance energy transfer strategies. Other NPs such as gold NPs (AuNPs) and carbonaceous NPs can be used as efficient fluorescence quenchers in fluorescence recovery approaches. In this case, fluorescently labeled probes are initially 'dark' because of their proximity to the NP surface. In the presence of target miRNA, the fluorophores are physically or chemically released from the NP and can emit fluorescence in a concentration-dependent manner. Last but not least, other properties such as the high surface area to volume ratio or the magnetic properties of NPs can be exploited for miRNA sensing. The detection strategies based on these properties are tagged 'unconventional' in the following paragraphs to distinguish them from the more classical optical detection schemes. A summary of the literature discussed in this section can be found in Supplementary Table 1, while in Figure 1 a classification of the strategies according to detection mode and chosen amplification strategy is shown.

AgNCs: optical detection

AgNCs produced by nucleic acid templated synthesis [44] are very small NPs (~1 nm or less) composed by a few silver atoms displaying a wide emission range (from UV to the near-IR region), outstanding photostability and high fluorescence efficiency [45]. AgNCs have been used for miRNA detection since 2011 as described by Yang and Vosch [46]. More recently, the Yang group has explored different design strategies to implement DNA-templated fluorescent AgNCs into miRNA quantification [47–49]. The common features of these approaches are: the miRNA recognition sequence and the AgNC-templating sequence and parts of the same oligonucleotide, and miRNA recognition results in fluorescence reduction in a concentration-dependent manner. Although throughout these attempts the measurable miRNA concentrations were found in the range from micromolar to nanomolar and thus probably too high to be of general use for miRNA quantification in biological samples (see Table 1), the efforts from Yang and coworkers contribute in understanding the factors governing the formation of fluorescent DNA-templated AgNCs.

Currently, the best way to lower the limit of detection (LOD, see Box 1) using AgNCs as the fluorescence reporters is to implement distinct oligonucleotides as the miRNA recognition sequence and the AgNC-templating sequence and to include an amplification step in the assay strategy. Ye and co-workers exploited target-assisted isothermal exponential amplification combined with DNA-scaffolded AgNCs [55,56]. This strategy was used for the concomitant quantification of miR-21 and miR-141 in cancer cell lysates with a remarkable LOD of 100 zmol (10 fM in 10 μl target-assisted isothermal exponential amplification reaction mixture). The method developed by Dong *et al.* is based on three oligonucleotides, in other words, a hairpin probe loaded with Hg^{2+} ions, an 'assistant' probe and an AgNC-templating sequence, used in combination with a nicking endonuclease enzyme (Nt.BbvCI) [57]. This assay allows also an LOD

of approximately 100 zmol (~1 fM in 100 µl assay mixture). However, no data were reported about miRNA quantification in samples of biological origin. The detection strategy developed by Zhang *et al.* exploited another peculiar photophysical property of DNA-templated AgNCs, namely the fluorescence enhancement of DNA-encapsulated AgNCs produced by the vicinity of a guanine (G)-rich DNA sequence [58]. This phenomenon was coupled to a strand displacement amplification reaction catalyzed by *Bsu* DNA polymerase. Yet, the assay was found to respond to miRNA concentrations only in the nM–µM range (an LOD of 2.5–5 pmol or 50–100 nM in 50 µl assay volume). Ye group proposed an interesting miRNA detection method in which enzymatic amplification is replaced by chemical amplification [59]. In particular, the target miRNA strands are sandwiched between magnetic microparticles (MMPs) and copper oxide (CuO) NPs, each of which decorated with DNA capture probes (CPs) complementary to a portion of the miRNA sequence. The sandwich complexes are isolated by application of an external magnetic field, followed by dissolution of the CuO NPs with diluted nitric acid to release Cu^{2+} in solution. Next, the solution is added of mercaptopropionic acid (MPA), which, under aerobic conditions, can be oxidized to the corresponding disulfide catalyzed by Cu^{2+}. Finally, detection is achieved by adding a fixed amount of preformed, fluorescent DNA-templated AgNCs, whose fluorescence is strongly quenched with increasing concentration of MPA, but not of disulfide. Thus, low miRNA amounts result in high MPA concentration and therefore in high fluorescence quenching, while high miRNA amounts result in low residual MPA (via oxidation) and high fluorescence. Signal amplification originates by one single CuO NP been made of up to 10^5 Cu^{2+} ions. However, the assay is multistep, requiring the isolation of the sandwich MMP–miRNA–CuO NP complexes. The LOD was found to be approximately 1 pM but no indication was given about the volume of the samples from which the miRNA is extracted in the form of a sandwich complex. The assay was used to quantify miR-221–5p in cancer cell lysates.

AuNPs: optical detection

AuNPs are among the most used nanomaterials for the development of *in vitro* diagnostic systems and biosensors because of their specific optical properties, which include localized surface plasmon resonance (LSPR), nanomaterial surface energy transfer and surface enhanced Raman scattering (SERS) [41].

Degliangeli *et al.* reported a real-time fluorescence recovery strategy for miRNA quantification based on enzymatic processing of DNA probes immobilized on PEGylated AuNPs [60]. The fluorescence of FAM-labeled DNA probes is initially quenched via nanomaterial surface energy transfer by the proximity to the gold surface. Upon hybridization with target miRNA, DNA:miRNA heteroduplexes are formed and become substrate of the enzyme duplex-specific nuclease (DSN), which selectively cleaves the DNA strand leaving the miRNA untouched resulting in target recycling ampli-

Table 2. Advantages and limitations of current miRNA quantification methods.

Method	Advantages	Limitations
Northern blot	• Quantitative • Direct information about miRNA size (iso-miR)	• Large amounts of RNA • Low throughput
qRT-PCR	• Quantitative • Small amounts of RNA • High sensitivity due to target amplification	• Medium throughput • The correct choice of an internal standard for normalization may be problematic • No possibility of discovering new miRNAs
Microarrays	• High throughput • Hundreds of miRNA sequences measured simultaneously	• Only semiquantitative information • No possibility of discovering new miRNAs • Lower specificity than qRT-PCR
RNA sequencing (next-generation sequencing)	• High throughput • High sensitivity and specificity • Can be used to discover new miRNAs	• High costs • Laborious data analysis requiring substantial specific computational knowledge • Absolute miRNA quantification not possible
Bead-based technologies (xMAP®: Luminex, Firefly® particles: Firefly BioWorks, and nCounter®: NanoString Technologies)	• Medium to high throughput • Hybridization takes place in solution	• No possibility of discovering new miRNAs • Low specificity for highly similar miRNAs, especially if the sequence variations are at the 5′ end • Limited comparative information available

qRT: Quantitative reverse transcription.

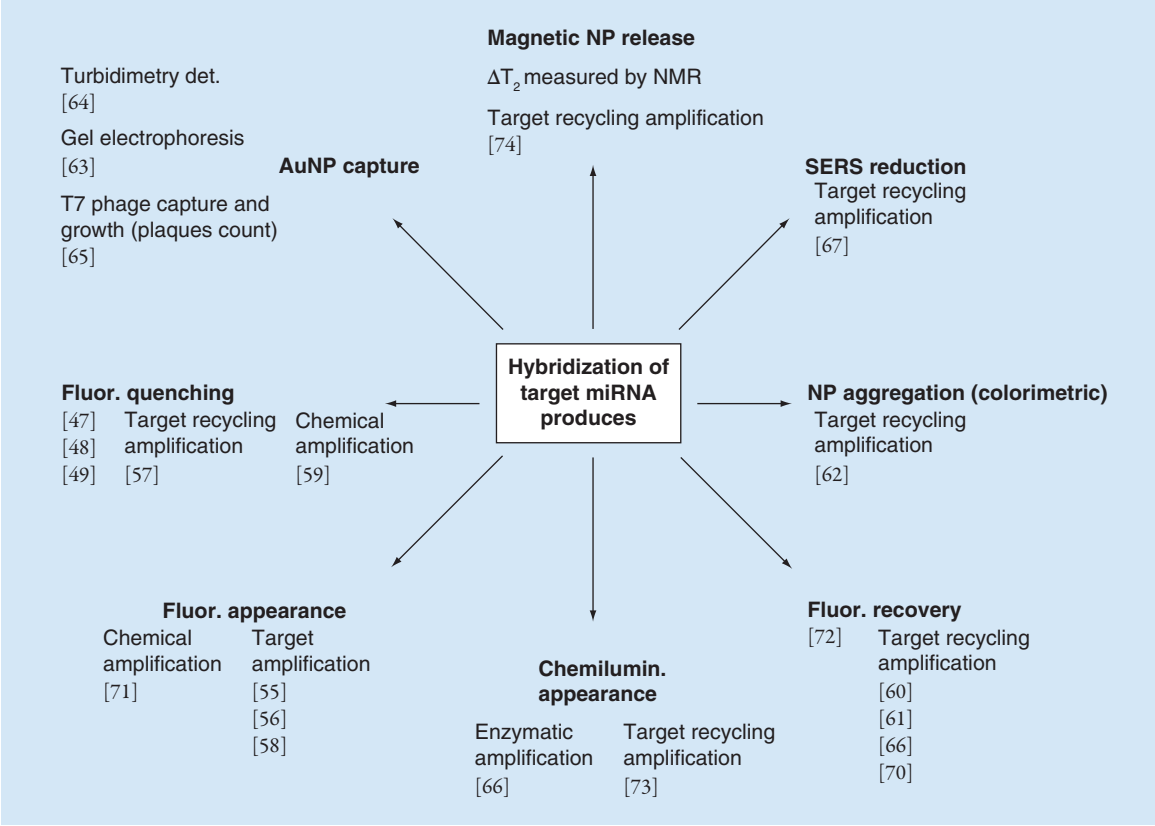

Figure 1. Quantification strategies based on nanoparticulate materials reviewed in this work. Classification is according to detection mode and signal amplification strategy.
NMR: Nuclear magnetic resonance; NP: Nanoparticle.

fication. DNA-probe hydrolysis results in fluorescence recovery due to the release of the fluorophores in solution (Figure 2).

The LOD for this approach is approximately 200 amol miRNA (or ~5 pM in 40 µl assay mixture). This assay was used for the quantification of miR-21 and miR-203 in extracted total RNA samples from cancer cell lines. Interestingly, the authors directly investigated the signal amplification contribution generated the DSN enzyme (Evrogen, Moscow, Russia) and found that at low miRNA concentrations approaching the LOD (<10 pM), the extent of this contribution to signal generation was relatively small (2–4 cleaved DNA probes/RNA).

Fluorescence recovery and DNA functionalized AuNPs are also exploited in the strategy developed by the Ma group [61]. Multiple QDs (the fluorescence emitters) are tethered to the surface of DNA-functionalized AuNPs via a DNA linker resulting in quenched fluorescence. Hybridization of target miRNA triggers the release in solution of the QDs with concomitant fluorescence recovery. The system is designed to incorporate nonenzymatic target recycling amplification based on strand displacement involving a single-stranded 'fuel' oligonucleotide, whose function is to release the target miRNA. The LOD was estimated to be approximately 500 amol (or 5 pM in 100-µl assay mixture). This assay was used for the quantification of miR-21 in extracted total RNA samples but also on living cells after concomitant intracellular delivery of QD–AuNP constructs and fuel oligonucleotides mediated by the transfection reagent Lipofectamine® 2000.

The colorimetric strategy reported by Ye group exploits the DSN enzyme and AuNP aggregation as transduction mechanism [62]. The assay is multistep and requires in the first step the enzymatic reaction on sample solutions supplemented by a DNA 'probe complex' of specific design, then quenching of the enzyme and finally addition of DNA-functionalized AuNPs for colorimetric detection. The LOD of this strategy is estimated approximately 400 amol (or 20 pM in 20-µl assay mixture, instrumental detection) and was applied to the quantification of miR-122 in cell lysates from human cancer cell lines.

AuNPs: unconventional detection strategies

The quantification strategy reported by Lee *et al.* takes advantage of AuNPs only as carrier material for signal amplification [63]. In fact, the assay strategy involves AuNPs functionalized with barcode DNA strands complementary to a portion of target miRNA and MMPs

Box 1. Limit of detection and limit of quantification

- Limit of detection (LOD): lowest amount of analyte in a sample that can be detected with a stated probability, although perhaps not quantified as an exact value [50]
- Limit of quantification (LOQ): lowest amount of analyte in a sample that can be quantitatively determined with a stated acceptable precision and trueness under stated experimental conditions [50]
- The assessment of a novel analytical method necessarily requires the estimation of the LOD and the related LOQ. Despite the common use and general understanding of the two terms, the appropriate estimation of these quantities has been controversial. However, there are reference documents describing internationally recognized and recommended procedures for meaningful LOD estimates [50–52]
- These procedures support the practitioner in correctly designing studies for LOD assessment, describe the assumptions, the statistical models underlying data treatment, and the interpretation of the results. A too often neglected recommendation is that a reliable estimate of the LOD requires repeated measurements on samples with relevant, low concentration of analyte and not only blank samples. In fact, for estimates based only on blank samples, there is no objective evidence that at low concentration the analyte will indeed produce a signal distinguishable from a blank (zero concentration) sample with a stated probability. Therefore, this approach 'defines only the ability to measure nothing' [53]. Furthermore, blanks and low level samples must be designed to account for matrix effects. The LOQ is generally derived from the LOD under given statistical assumptions which need to be verified [54]

LOD: Limit of detection; LOQ: Limit of quantification.

functionalized with DNA strands complementary to the rest of the miRNA sequence. In the presence of target miRNA, AuNPs are captured by the MMPs forming a sandwich complex. The complexes are isolated by the application of a magnetic field, denatured to release the barcode DNA-functionalized AuNPs followed by complete chemical etching of the gold core with KCN and release of the barcode DNA strands in solution. Upon addition of complementary oligonucleotides, double-stranded DNAs are formed and analyzed by gel electrophoresis on a native polyacrylamide gel. Each miRNA gives rise to a separate band according to the size of the coding DNA sequence; thus, this strategy holds the intrinsic possibility of multiplexing. Although detection of miRNA is greatly enhanced because each AuNP carries approximately 1500 barcode DNA strands and just 1 miRNA molecule is sufficient for the immobilization of 1 AuNP, quantification is complicated by a nonlinear response to miRNA concentration. An additional concern is the use of highly toxic cyanides in the assay.

Chen *et al*. also employed the multivalency of DNA-functionalized AuNPs as a mean to amplify the detection signal [64]. Their visual detection strategy is based on the formation of MMP–AuNP–polymer microparticle ternary complexes hold together by DNA complementary strands. These complexes are the final product of a multistep procedure whereby the amount of AuNPs, and thus of sandwich complexes, reflects the initial amount of target miRNA. Upon application of a magnetic field in the detection step, the complexes are removed from the solution and the remaining turbidity (due to the excess of polymer microparticles) inversely correlates with the amount of miRNA, in other words, high turbidity indicates low miRNA and vice versa. The assay was used to detect miR-155 on total RNA extracted from cultured cancer cells.

Zhou *et al*. developed a visual detection strategy based on the naked eye counting of fluorescent plaques in a Petri dish containing a host bacterial medium (Figure 3) [65]. The appearance of plaques is due to infection of the bacteria by an engineered T7 phage. According to the design strategy, the number of observed plaques should be the same as the number of phages and to the number of target miRNA. AuNPs are essential components of this assay. In fact, the strategy requires DNA-functionalized AuNPs and MMPs, and a T7 phage expressing gold-binding peptides near the tips of the six tail fibers as well as enhanced green fluorescent protein or red fluorescent protein on the capsid. In the presence of target miRNA, preformed 1:1 AuNP/T7 phage constructs are assembled on the surface of MMP via sandwich hybridization. This multistep strategy, which includes a CsCl gradient centrifugation to isolate the 1:1 AuNP/T7 phage constructs, was found to be applicable for the quantification of miRNA into spiked human serum samples. In all tested cases, the capturing efficiency was found approximately 50%, in other words, the number of observed plaques is approximately half the expected number of miRNA molecules. This strategy is suitable only for counting miRNAs at less than fM concentrations owing to the limited capacity to accommodate plaques in a Petri dish.

QDs: optical detection

The miRNA quantification strategy developed by Jou *et al*. exploits DNA-functionalized semiconductor QDs as essential transduction element [66]. The DNA-probe strands immobilized on the QD surface carry a Black Hole Quencher® dye (BHQ-2 [Biosearch Technologies,

CA, USA]) strongly reducing QD emission. In the presence of target miRNA, heteroduplexes are formed and become substrate of the DSN enzyme. The possible amplification factor due to miRNA recycling is however limited by the low number of DNA strands on each QD (~8) and by the fact that each tethered BHQ-2 unit contributes only partially to the quenching of the total QD fluorescence. Nevertheless, the lowest measured miR-141 concentration was 1 pM (or 5 amol in 5 µl miRNA solution) but under the used experimental conditions the method was found to have poor selectivity. The selectivity of the method could be greatly enhanced by coupling a second enzymatic step after DSN digestion. In particular, only the digested probe strands obtained from miR-141:DNA probe heteroduplexes (and not those from other miRNAs) can work as primers for the telomerase enzyme. Thus, telomerase extension functions as an additional discriminating event but also allows further amplification. In fact, telomeric chains self-assemble into G-quadruplexes and originate peroxidase-mimicking DNAzyme units upon hemin binding. Finally, addition of hydrogen peroxide and luminol results in a chemiluminescence signal used as readout for miR-141 quantification in the complete assay. This approach was used to measure miR-141 levels in the extracted small RNA fraction from the serum of prostate cancer and healthy patients.

Other NPs: optical detection

In a very recent report, Pang *et al.* proposed DNA-functionalized Fe_3O_4@Ag core–shell magnetic NPs for miRNA capture and DSN signal amplification to be detected via SERS spectroscopy [67]. Detection occurs in a separate step following magnetic separation of the DSN-treated Fe_3O_4@Ag. The presence of target miRNA produces an attenuation of the SERS signal (Figure 4).

The LOD of this strategy is excellent and corresponds to 15 zmol miRNA (0.3 fM in 50-µl assay mixture). Although this approach may allow miRNA quantification in samples with low miRNA content (e.g., body fluids; see Table 1), only quantification of let-7b in total RNA extracted from cultured cancer cells was reported.

Recent years have seen an enormous interest in the use of carbonaceous NPs for sensing application. Single-stranded fluorescently labeled DNA probes can adsorb on the surface of graphene and graphene oxide (GO) resulting in efficient fluorescence quenching [68,69]. In the presence of complementary oligonucleotides (e.g., target miRNA), duplexes are formed and released in solution resulting in fluorescence recovery. Robertson *et al.* employed nanoscale graphene oxide (nGO) to develop an miRNA quantification strategy mainly focusing on the discrimination of miRNA sequences with a single mutation [70]. Their assay includes an enzymatic step catalyzed by DNAse I for miRNA target recycling and the grafting of poly(ethylene glycol) methyl ether methacrylate polymers to the nGO edges to abolish the background and improve selectivity. Bi *et al.* exploited the use of MMP/nGO composites combined with a cascaded chemiluminescence resonance energy transfer (C-CRET) mechanism for signal detection [71]. This system is composed of a hairpin probe whose opening, upon target recognition, is responsible for abolishing quenching via CRET and appearance of a fluorescence signal. The assay is discontinuous but the system is regenerable and generally applicable to any miRNA sequence. The lowest measured miRNA concentration is 100 pM in 150-µl hybridization mixture (15-fmol miRNA).

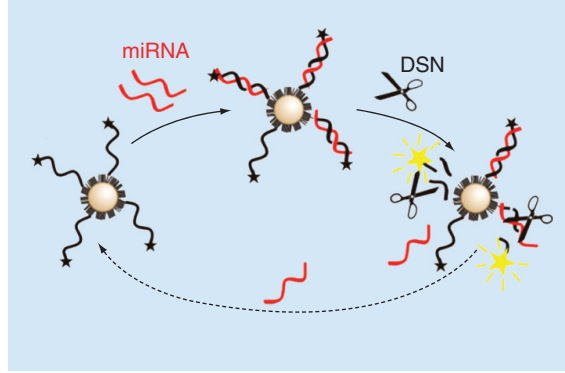

Figure 2. Target miRNA hybridizes to fluorescently labeled DNA probes immobilized on PEGylated gold nanoparticles. The DNA strands of the heteroduplexes are selectively hydrolyzed by DSN generating a fluorescence signal due to release of the fluorophores. The signal is amplified via recycling of the intact miRNA target.
DSN: Duplex-specific nuclease.
Reprinted with permission from [60] © American Chemical Society (2014).

Other organic and metal–organic materials have been recently tested in miRNA detection as fluorescence quenchers [72,73], although with no major advantage compared with carbonaceous NPs.

Other NPs: unconventional detection strategies

Lu and coworkers reported a very sensitive miRNA quantification assay which exploits the change of transverse relaxation time (ΔT_2) of water molecules as the physical readout [74]. The assay's principle is as follows: MMPs of approximately 1-µm diameter (MM_{1000}) and 30-nm magnetic NPs (MN_{30}) are assembled into MM_{1000}–DNA–MN_{30} conjugates using heterobifunctional DNA probe strands (amino modified at 5′ end and biotin modified at 3′ end) as linkers. These conjugates display on average approximately 300 MN_{30} on the surface of each MM_{1000} bead. In the presence of miRNA,

heteroduplexes are formed and hydrolyzed by the DSN enzyme releasing MN_{30} in solution. As earlier noted, this enzyme allows signal amplification via miRNA target recycling. After a fixed time, the released MN_{30} can be efficiently separated from the much larger MM_{1000} by applying a 0.01-T magnetic field for 3 min. This field strength leaves MN_{30} well dispersed in the assay mixture because of their low saturation magnetization. Finally, the ΔT_2 of water molecules in the supernatant containing the dispersed MN_{30} is measured using a 1.5-T nuclear magnetic resonance spectrometer. It was found that the ΔT_2 values increase with the logarithm of miRNA concentration, which correlates with increasing number of MN_{30} in solution. The method allows a remarkable LOD of around 150 zmol miRNA (5 fM in 30-µl assay mixture) and was applied to the quantification of miR-21 in total RNA extracted from cancer cell lines as well as from tumor tissues. Nevertheless, the sensitivity of the method is only moderate with ΔT_2 varying approximately 100 ms for each order of magnitude of miRNA concentration. Despite the very good LOD of this approach, quantification of low abundance miRNAs or quantification of endogenous circulating miRNAs (e.g., in serum or other body fluids) was not demonstrated.

Strategies based on nanostructured surfaces

Quantification strategies based on solid supports are attractive for practical reasons such as robustness, portability and storage simplicity. Substrate nanostructuration directly contributes to signal transduction, for example, plasmon-enhanced fluorescence (PEF), as well as to device miniaturization. The most recent

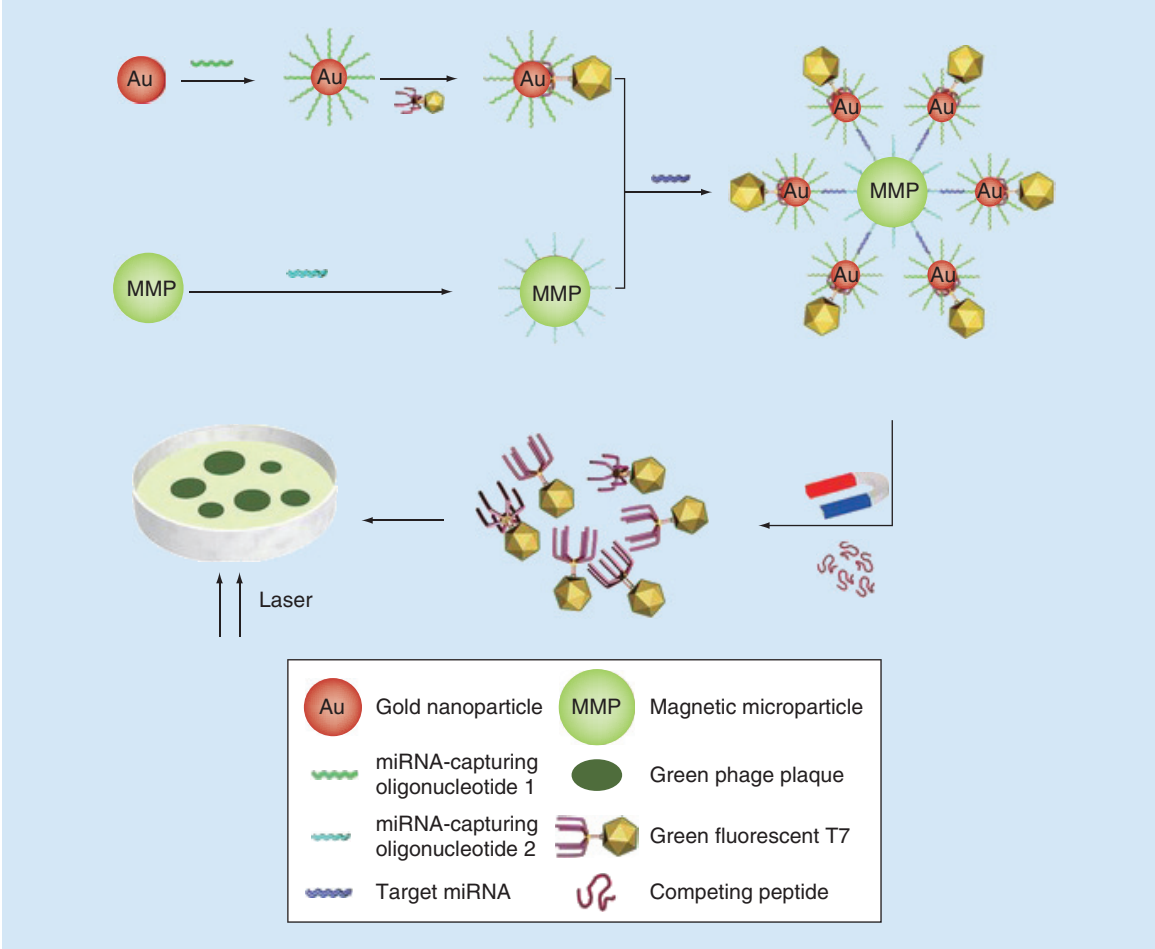

Figure 3. Quantification of miRNAs based on the naked eye counting of fluorescent plaques in a Petri dish. The 1:1 AuNP/T7 phage assemblies are captured on magnetic microparticles in the presence of target miRNA; removal of excess AuNP/T7 phage assemblies, followed by T7 phage release from AuNPs driven by treatment with a competing peptide; the phages are finally used to infect a host bacterial medium and their reproduction produces colored/fluorescent plaques. Each plaque corresponds to one phage and to one miRNA. The overall counting efficiency is estimated around 50%, in other words, the number of visualized plaques is approximately half of the number of miRNA strands in the sample.
Reprinted with permission from [65] © Macmillan Publishers Ltd: Nature Materials (2015).

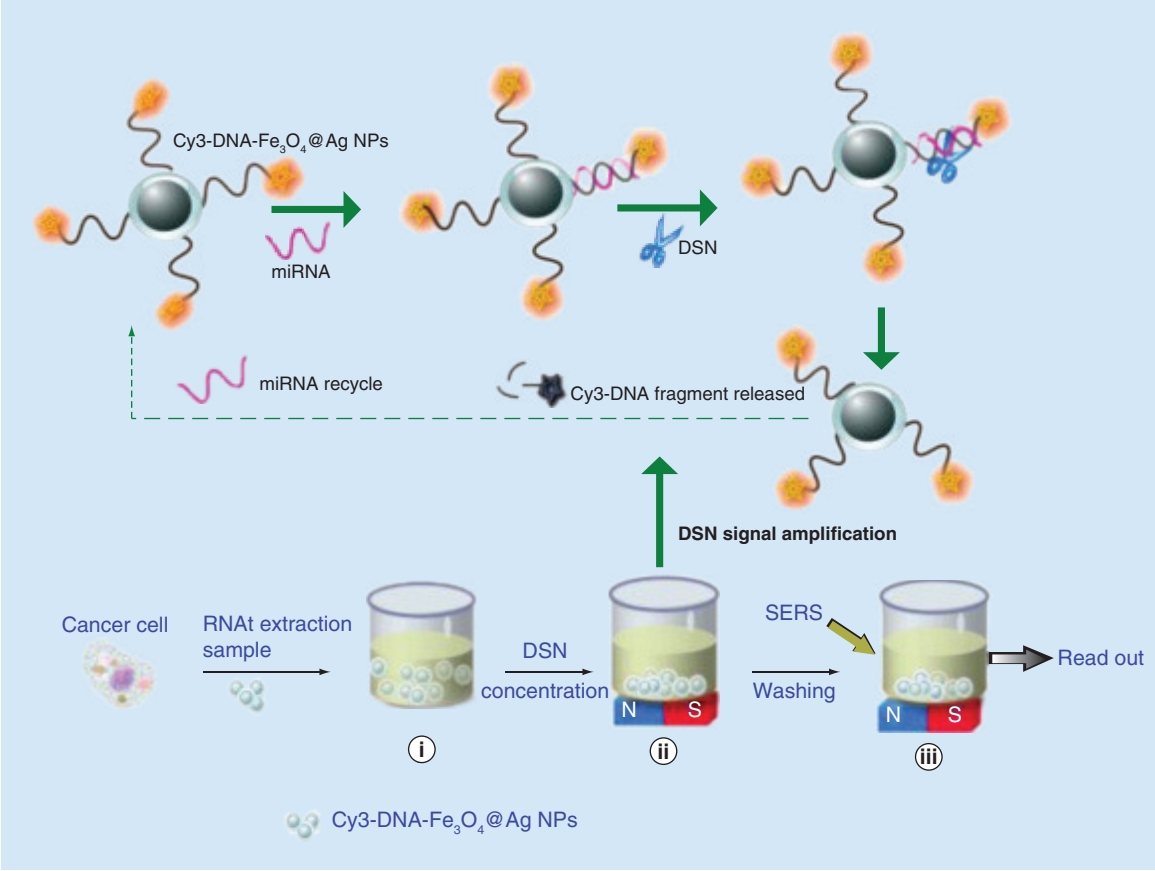

Figure 4. DNA-functionalized Fe_3O_4@Ag core–shell magnetic nanoparticles for miRNA quantification. Fluorescent dyes labeling the DNA probe strands are in the vicinity of the Ag surface and produce a SERS signal. In the presence of target miRNA, heteroduplexes are formed and the DNA strands cleaved by the DSN enzyme, producing the release of fluorophores and a consequent loss of SERS signal. The intact miRNA can initiate the cleavage of another DNA-probe strand increasing the magnitude of signal reduction. Total RNA is incubated with the Fe_3O_4@Ag NP probes **(i)**. The NPs are then magnetically concentrated before DSN treatment **(ii)**. The NPs must be washed to remove the Cy-3-DNA fragments in solution before reading out the final Raman signal **(iii)**.
DSN: Duplex-specific nuclease; NP: Nanoparticle; SERS: Surface enhanced Raman scattering.
Reprinted with permission from [67] © Elsevier (2016).

literature describing miRNA quantification based on nanostructured surfaces focuses on optical detection (direct or interferometric) and is summarized in Supplementary Table 2.

Optical detection

The Liu group described an optical detection strategy made possible by the combination of PEF with hybridization chain reaction (HCR), an enzyme-free amplification strategy [75]. In particular, a plasmonic chip on a glass surface was fabricated by producing nanostructured gold islands with abundant nanogaps for electromagnetic field enhancement to improve PEF detection. The gold surface was functionalized with locked nucleic acid probes complementary to one part of the target miRNA. The adjacent part of the miRNA sequence is recognized by an azide-modified locked nucleic acid trigger probe, which is able to initiate HCR in the presence of two azide-modified DNA hairpins. Finally, the surface immobilized HCR product is labeled with near-IR fluorescent dyes (cyanine-5, Cy5) via copper-free click chemistry involving the azido groups. The fluorescence of the immobilized dyes is largely enhanced by the PEF phenomenon. The lowest measured concentration of miR-21 using this multistep approach, which includes a denaturing step at 95°C, was 1 fM (50 zmol in 50-µl sample volume). The assay was applied to the quantification of miR-21 in extracted total RNA from cancer cell lines. The ability to measure very low miRNA concentration was further demonstrated by reducing the amount of total RNA in the assay to as little as that corresponding to only five cells. The specificity of the assay under the reported conditions is only moderate.

An optical sensor based on a Mach–Zehnder interferometer (MZI) with a slot waveguide configuration was

reported by Liu *et al.* [76]. The MZI biosensor was fabricated using standard micro-nanofabrication techniques typical of complementary metal-oxide-semiconductor processes. These processes enable a larger number of sensors to be integrated on the same chip and therefore this technology is ideally suited for miRNA multiplexing analysis. In practice, each MZI sensor on the chip can be functionalized with a different DNA probe using a microarray spotter and the response to each miRNA target can be monitored simultaneously. In essence, for each MZI sensor, the incoming waveguide splits into two arms called reference arm and sensing arm, and recombines again after a certain distance before the detector (an IR GaAs camera). The surface of the sensing arm is functionalized with DNA probes and is in contact with the sample solution. In the presence of target miRNA, formation of miRNA:DNA heteroduplexes determines a phase change ($\Delta\Phi$) between the light beam emerging from the sensing arm and the light beam emerging from the reference arm. Recombination of the two light beams produces interference and results in a measurable change in light intensity, which can be used to calculate ($\Delta\Phi$). This physical parameter was shown to vary proportionally to the base 10 logarithm of miRNA concentration. The lowest measurable concentration for this approach is quite high (~1 nM). However, it was possible to quantify miRNA in the small RNA-enriched fraction extracted from urine samples.

The Lechuga group developed a nanophotonic biosensor, based on interferometric bimodal nanowaveguides (BiMW) [77]. The essence of the BiMW device is a single channel waveguide interferometer able to produce the interference of two waveguide modes of the same polarization. This configuration avoids light beam splitting and recombination, which are necessary in the case of the previous MZI sensor. The sensing window of this device is situated along the bimodal section of the waveguide. Here, the evanescent electromagnetic field associated with the light beam propagating in the waveguide is in contact with the external medium and is sensitive to the refractive index variations of the environment. Since the two waveguide modes are differently confined,

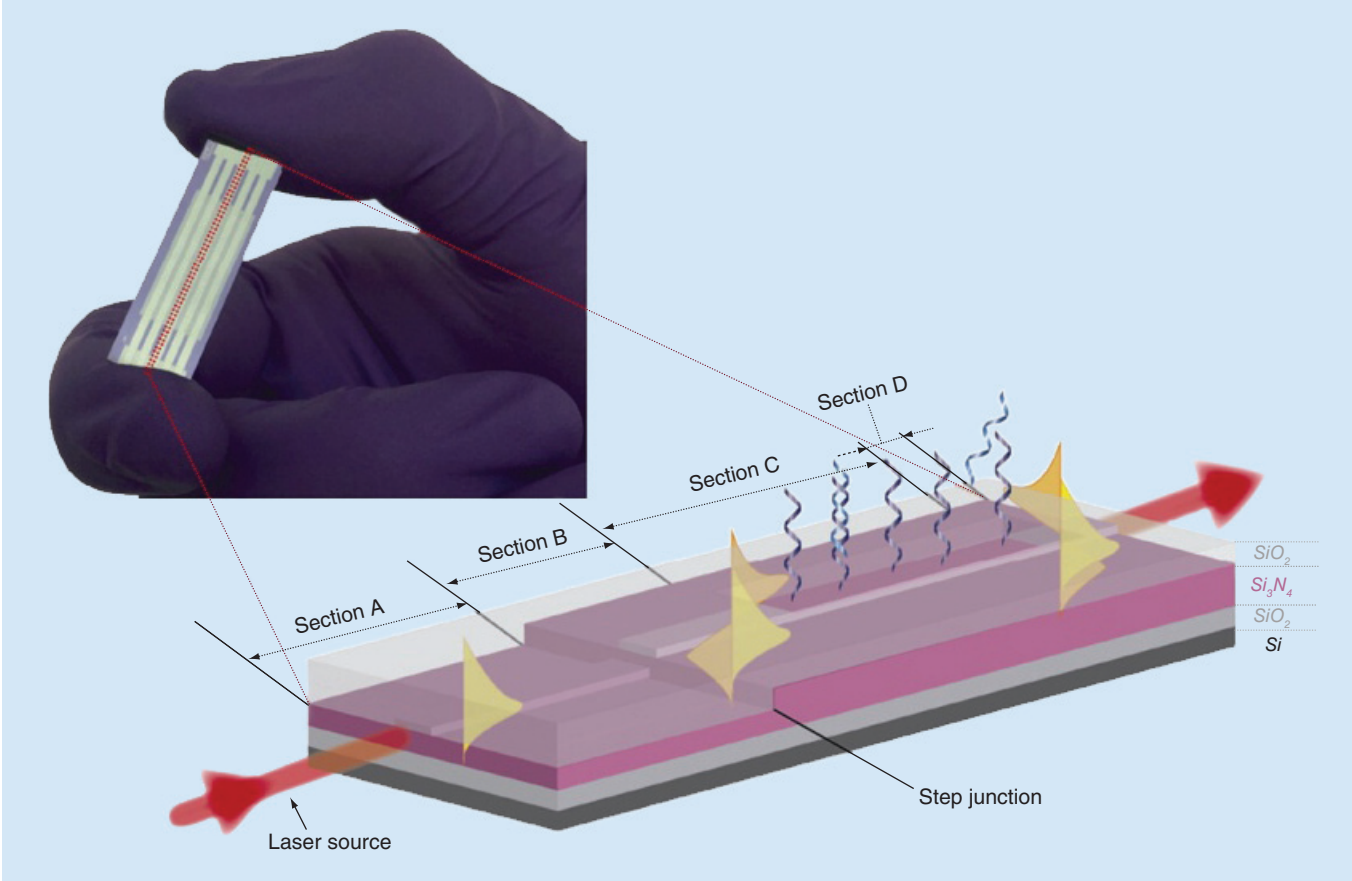

Figure 5. Schematic drawing and a photograph of the BiMW sensor. Transverse electric-polarized light is coupled in the waveguide in Section A. The fundamental propagation mode splits into two modes in Section B after the step junction. The sensing window of the device is labeled Section C. Here the miRNA probes are immobilized on the Si_3N_4 surface. A two-section photodetector is placed at the end of the waveguide in Section D.
Reprinted with permission from [77] © American Chemical Society (2016).

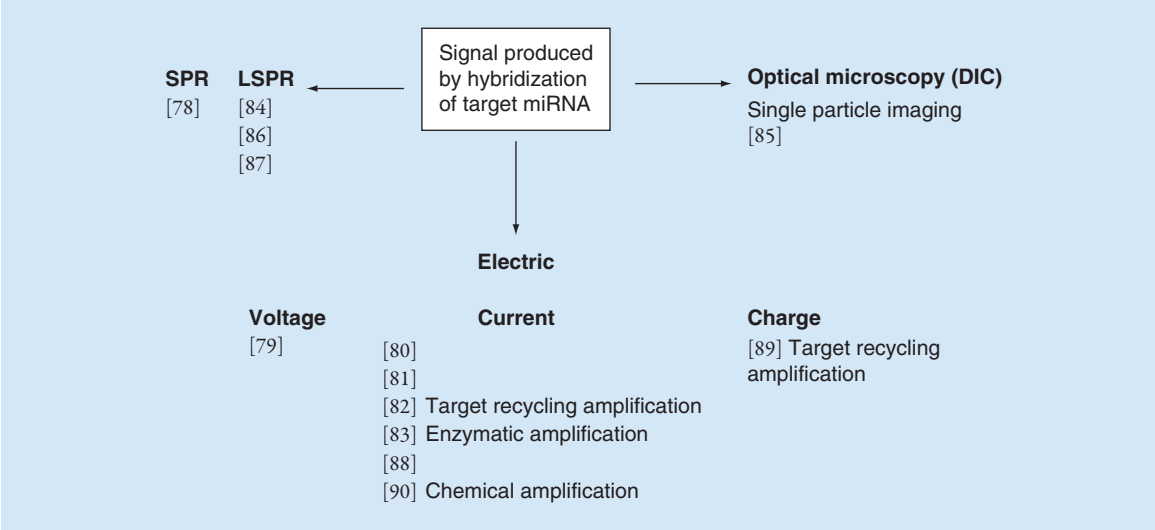

Figure 6. Quantification strategies based on the combination of surfaces with nanoparticulate materials reviewed in this work. Classification according to detection mode and signal amplification strategy.
DIC: Differential interference contrast; LSPR: Localized surface plasmon resonance; SPR: Surface plasmon resonance.

a phase difference accumulates along the propagation length giving rise to an interferometric signal which correlates with the amount of miRNA target binding to the DNA probes (Figure 5). In particular, it was found that the phase shift ΔΦ exponentially increases with increasing Log miRNA concentration and the LOD was estimated approximately 23 aM (or ~6 amol in the 250-µl sample injected over the BiMW sensor).

The possibility of measuring remarkably low miRNA concentration was exploited for the quantification of miR-181a directly in urine samples. Before loading on the sensor, the urine sample was diluted 1:1 (or better 1:10) with a high stringency hybridization buffer, which was developed and tested specifically in this work. Similar to the previously described approach, the BiMW fabrication technology is optimally suited for the preparation of sensor arrays and thus for multiplexing. The described BiMW sensors are equipped with a fluidic cell with four independent 15 µl volume channels, each of which addresses a group of four sensors.

Combination of surface strategies with nanoparticulate materials

The combination of nanoparticulate materials with solid supports is a simple and effective way to increase the surface area and to improve probe presentation/accessibility and can be exploited for the development of strategies with optical or electrochemical detection. A summary of the literature discussed in this section is reported in Supplementary Table 3, while Figure 6 reports a classification of the different strategies according to detection mode and chosen amplification strategy.

Composites based on carbonaceous NPs

GO–AuNP composites were proposed by Wang *et al.* as key elements for a detection strategy based on surface plasmon resonance (SPR) [78]. This strategy employs a gold film carrying DNA probes, whose sequence is complementary to a part of the target miRNA, and GO–AuNP composites where the AuNPs carry DNA probes complementary to the adjacent, remaining part of the miRNA. In the presence of miRNA, the GO–AuNP composites are immobilized on the surface by sandwich hybridization. The SPR signal is enhanced by the electronic coupling of the localized plasmon of AuNPs with the surface plasmon wave associated with the Au film. Since each GO–AuNP flake is composed of many AuNPs, additional amplification of the SPR signal is possible. The estimated LOD of this multistep assay was 1 fM.

A combination of reduced GO (R-GO) and AuNPs was exploited by Cai *et al.* for the development of a field-effect transistor (FET) based biosensor for miRNA detection [79]. Peptide nucleic acid probes were used as the recognition element immobilized on AuNPs decorating the R-GO layer. Hybridization of the target miRNA can be followed electrically and results in a shift in the gate voltage at minimum conductance when the transfer curve for the FET device is measured. This multistep assay reaches an estimated LOD of 10 fM. A R-GO–AuNP combination was also exploited by Cheng *et al.* for their electrochemical detection strategy [80]. DNA probes are immobilized on an R-GO–AuNP layer deposited on the surface of a glassy carbon electrode. Their sequence is complementary to half of the target miRNA. The sample solution in contact with the elec-

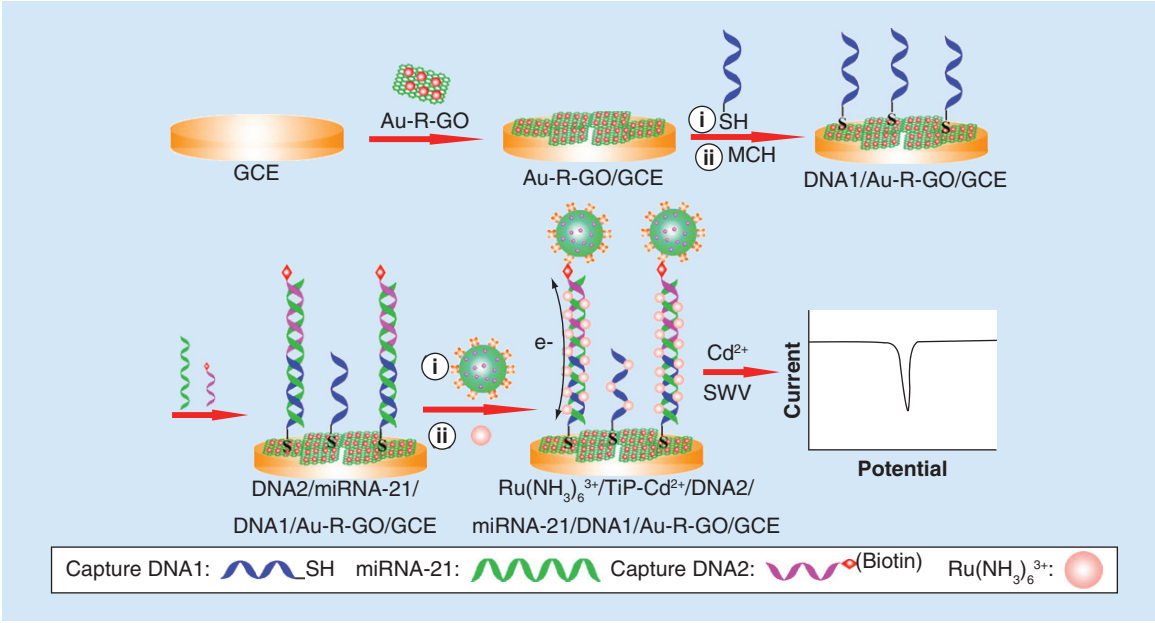

Figure 7. Ultrasensitive miRNA detection via square wave voltammetry. AuNP/R-GO nanocomposites are deposited on the surface of a glassy carbon electrode. DNA probes (capture DNA1) are then immobilized on the AuNPs in the composites. In a following step, target miRNA and a biotinylated DNA sequence (capture DNA2) are concomitantly immobilized via hybridization. Finally, streptavidinated Cd^{2+}-doped titanium phosphate nanospheres (TiP-Cd^{2+}) are recruited to the electrode surface. The fully assembled sensor is interrogated via SWV monitoring the peak current for Cd^{2+}. The large amount of Cd^{2+} ions incorporated into the TiP nanospheres is responsible for signal amplification and allows this approach to reach a record low LOD.
AuNP: Gold nanoparticle; GCE: Glassy carbon electrode; MCH: 6-Mercapto-1-hexanol; R-GO: Reduced graphene oxide; SWV: Square wave voltammetry.
Reprinted with permission from [80] © American Chemical Society (2015).

trode also contains biotin-labeled DNA reporters complementary to the other half of the miRNA. In the presence of target, the three oligonucleotides hybridize and recruit streptavidinated Cd^{2+}-doped titanium phosphate nanospheres (TiP-Cd^{2+}) to the electrode surface. Large amounts of Cd^{2+} ions are incorporated into the TiP nanospheres, providing high electrochemical signals. $Ru(NH_3)_6^{3+}$, which is known to bind to double-stranded nucleic acids, is added to enhance electron transport. Detection is achieved through square wave voltammetry monitoring the peak current for Cd^{2+} (Figure 7).

This multistep assay achieves a record low LOD of approximately 4 ymol miRNA (~0.8 aM in 5-µL sample volume) and was used for the direct quantification of miR-21 in serum of cancer patients and healthy individuals.

An electrochemical strategy was reported by Azimzadeh *et al.* who modified the surface of a glassy carbon electrode with a thin layer of GO decorated with DNA-functionalized gold nanorods [81]. The intercalating dye, Oracet Blue, was used to reveal the formation of miRNA:DNA probe hybrids via differential pulse voltammetry (DPV), whereby the intensity of the DPV current increases with miRNA concentration. Analogous to other electrochemical detection strategies [42], this assay is multistep and involves several washing steps which may affect reproducibility but achieves a very good LOD of approximately 5 zmol miRNA (~1 fM in 5-µl sample volume).

The combination of single-walled carbon nanotube (SWCNTs) and CdS (QDs) deposited on an indium tin oxide (ITO) transparent electrode was exploited by Cao *et al.* for the photoelectrochemical sensing of miRNAs [82]. In this proof-of-principle study, the authors showed that one-pot synthesized DNA–CdS QDs could be combined with carboxyl-functionalized SWCNTs through π–π stacking forming the photoelectrochemically active species. These composites exhibited high photovoltaic conversion efficiency and good stability. In the presence of target miRNA, heteroduplexes are formed and CdS QDs are released from the surface of SWCNTs, resulting in a measurable photocurrent reduction (Figure 8).

The signal was further amplified using DNAse I for target recycling. Under optimized conditions, an LOD of approximately 0.6 amol (~40 fM in 15-µl hybridization mixture) was estimated for this multistep assay using synthetic miRNAs in buffer. More recently, g-C_3N_4(graphitic carbon nitride)–AuNP composites on an ITO substrate were exploited for the photoelectro-

chemical detection of miRNA [83]. Probe DNAs immobilized on the g-C_3N_4–AuNP layer form DNA:miRNA heteroduplexes which are recognized by the S9.6 antibody, an anti-DNA:RNA antibody. Afterward, the immobilized antibody is recognized by a secondary antibody immobilized on AuNPs labeled with alkaline phosphatase. Alkaline phosphatase catalyzes the hydrolysis of ascorbic acid-2-phosphate in the detection solution to produce ascorbic acid which works as the electron donor. As a result, in the presence of target miRNA, a strong photocurrent is observed and its intensity increases with increasing amounts of miRNA. Note that this assay allows signal-on detection, as opposed to the signal-off detection of the previous strategy, but the number of steps necessary for biosensor preparation is increased.

AuNPs: optical detection

The Chen group reported the use of single-nanostructure spectroscopy to quantify miRNAs in extracted total RNA [84]. Their chip-based sensing platform is based on AuNP dimers linked by stem–loop DNA and anchored on a glass substrate. The loop sequence is complementary to the target miRNA. Upon miRNA binding, the AuNP dimer geometrically extends resulting in an energy change for the hybridized plasmon mode, detectable as a spectral shift of the scattered light. Single AuNP dimers, composed of one AuNP with 100-nm diameter and one 60-nm AuNP, are imaged and identified using an inverted microscope with a transmitted dark-field condenser taking advantage of their strong light scattering properties. Single AuNPs and other aggregates can be differentiated by analyzing the polarized scattered light. After identification of single dimers, the fractional spectral shift, defined as the wavelength change divided by the initial LSPR peak position ($\Delta\lambda/\lambda$), of each dimer is measured. Data from 25–65 dimers undergo statistical analysis to obtain the average fractional shift, which was found to vary linearly with the logarithm of miRNA concentration up to 0.1 pM. The LOD estimated for this strategy is approximately 0.6 amol (or ~9 fM in 60-µl sample volume), and it was possible to quantify variation of miR-210 levels in total RNA extracted from normoxic versus hypoxic cells. Although this method is still rather laborious from the point of view of data acquisition and data analysis, and displays a relatively narrow working range, it holds good potentiality in terms of achieving multiplexed arrays with ultrahigh density for biomarkers profiling.

The strategy developed by the Ying group is also based on optical detection of AuNPs on a glass surface and is intrinsically amenable to multiplexing [85]. They fabricated a microarray of hairpin CPs, the loop of which is complementary to the target miRNA. The DNA hairpins are opened up as a consequence of miRNA hybridization exposing a 'universal' single-strand DNA sequence which can hybridize with the signaling probes on 5-nm diametered AuNPs. Thus AuNPs are captured on the surface via formation of DNA (CP):miRNA:DNA (sig-

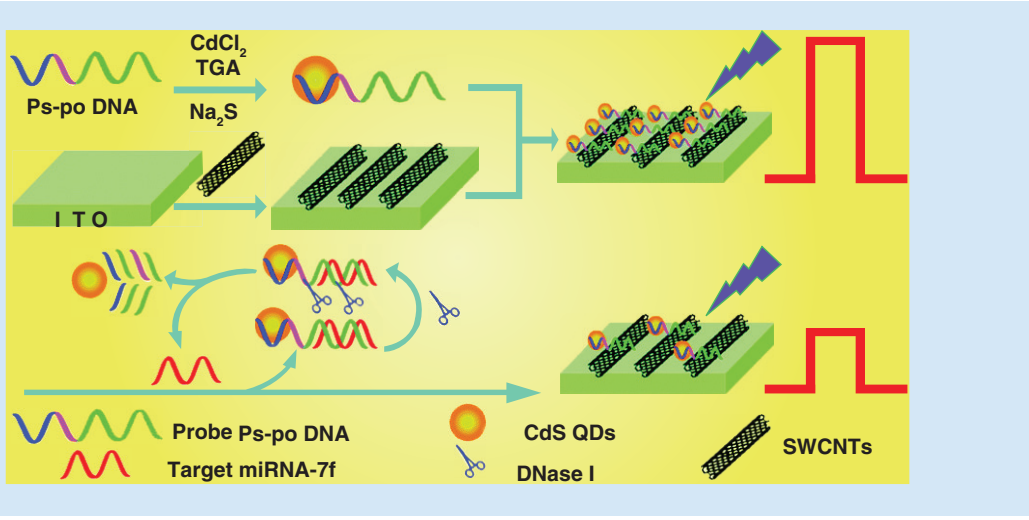

Figure 8. Photoelectrochemical detection of miRNA. DNA–CdS quantum dots are adsorbed on the surface of single-walled carbon nanotube on a transparent indium tin oxide substrate. Irradiation at 405 nm produces a strong photocurrent. In the presence of target miRNA, hybridization triggers the release of DNA–CdS QDs in solution and a consequent reduction in the observed photocurrent upon irradiation. The release of DNA–CdS QDs (and thus the photocurrent reduction) can be magnified via target recycling using the enzyme DNAse I.
ITO: Indium tin oxide; QD: Quantum dot; SWCNT: Single-walled carbon nanotube; TGA: Thioglycolic acid; Ps-po DNA: DNA probe with one part of the sequence based on phosphorothioate internucleotide linkages and one part on natural occurring phosphodiester linkages.
Reproduced with permission from [82] © The Royal Society of Chemistry.

naling probe) sandwich complexes and imaged by differential interference contrast (DIC) microscopy. The number of immobilized AuNPs visualized by DIC was found to be proportional to the logarithm of miRNA concentration. The LOD of this strategy was found to be 0.2 amol (10 fM in 20-µl sample solution during hybridization) but increased to 2 amol when human serum was analyzed.

The groups of Korc and Sardar developed a plasmonic biosensor for the detection of miRNAs in biological fluids [86,87]. The sensor is based on gold nanoprisms attached onto a glass substrate which are functionalized with DNA probes. Binding of target miRNA produces a shift of the LSPR peak measured by UV–VIS spectroscopy. The magnitude of this shift increases linearly with the logarithm of miRNA concentration. The LOD for miR-21 in simulated samples containing 40% bovine plasma or 40% human plasma was approximately 28 amol (~35 fM in 800-µl sample solution during hybridization) [86]. This sensor could be used to quantify miR-21 and miR-10b in human plasma samples collected from pancreatic ductal adenocarcinoma patients. Interestingly, the authors demonstrated that the sensor surface can be regenerated through several cycles by treatment with RNAse H. Some limitations of this strategy include the required long hybridization time (12 h), its multistep implementation and its relatively low sensitivity (defined as the slope of the $\Delta\lambda_{LSPR}$ vs log[miRNA] curve). In a following report, the authors demonstrated a >400-times improvement in LOD (~80 aM or ~64 zmol considering a 800-µl sample volume during hybridization as in the previous report) by finely tuning the dimensions of the Au nanoprisms [87].

AuNPs: electrochemical detection

The Ding group reported an electrochemical sensor constituted by self-assembled 3D DNA origami nanostructures with a tetrahedron shape anchored on to a layer of AuNPs deposited on a bare gold disk electrode [88]. The DNA tetrahedra display at their apex a stem-loop portion which is tagged with an electroactive ferrocene moiety. Upon miRNA binding, the loop is opened and the overall flexibility of the structure is increased allowing the ferrocene groups to contact the electrode surface resulting in an increased electrochemical signal. Increasing miRNA concentrations results in increasing peak currents measured by DPV. In particular, the measured current varies linearly with the logarithm of miRNA concentration (from 100 pM to 1 µM).

The strategy described by Miao *et al.* [89] is based on chronocoulometry, a classical electrochemical technique where the charge (coulombs) is measured as a function of time. In their approach, DNA probes are immobilized on the surface of a gold electrode. In the presence of target miRNA, heteroduplexes are formed and can be selectively cleaved by the DSN enzyme resulting in amplification via target recycling. After a fixed time (2 h), the electrode is rinsed and treated with DNA-functionalized AuNPs, whose sequence is complementary to the DNA-probe sequence. Thus, the number of AuNPs that can be immobilized on the electrode surface is high for low miRNA concentrations, corresponding to low amounts of DSN-hydrolyzed probes, and low for high miRNA concentration. Finally, the electrode is again rinsed and transferred to the electrochemical cell for chronocoulometry measurements. The redox charge of the electrode decreases linearly with increasing the logarithm of miRNA concentration. The LOD of this assay for miR-29a-3p was estimated 50 aM.

The cyclic voltammetry approach reported by the Ma group consists of DNA CPs immobilized on the surface of a gold electrode and methylene blue labeled, G-rich DNA detection probes immobilized on AuNPs [90]. In the presence of target miRNA, sandwich complexes can be formed resulting in the recruitment of AuNPs to the electrode surface. The G-rich DNA detection probes are designed to fold into G-quadruplexes in the presence of K^+ ions and bind an electrochemically active Ir(III) complex. Detection by cyclic voltammetry occurs in the presence of H_2O_2 monitoring the current intensity corresponding to the methylene blue reduction peak as a function of miRNA concentration. AuNPs are essential for signal amplification because each NP carries many G-rich DNA detection probes which can bind the electrochemically active Ir complex. As little as 10-fM miR-21 could be quantified in spiked human serum samples.

Conclusion & future perspective

Quantification of miRNA expression levels is expected to give a major contribution to cancer diagnosis and prognosis in the coming years. However, there are still several technological and methodological aspects related to miRNA quantification which need to be improved. In general, there is still an urgent need for standardization in every aspect of miRNA quantification including the discovery of relevant miRNA panels; the validation of the most appropriate specimen; the sampling, storage and specimen processing procedures (preanalytical variables); and the actual analytical and data normalization procedures. Some of the limitations of currently most used standard technologies, that means, northern blotting, qRT-PCR, microarrays and NGS, derive from having adapted standard methods developed for the quantification of other classes of nucleic acids (e.g., DNA and mRNA) to the analysis of miRNAs. Therefore, there is a great interest in developing new strategies for improving the accuracy, specificity, sensitivity and LOD of miRNA quantification.

Nanotechnology can provide advanced materials and surfaces to successfully address this analytical problem. In fact, nanotechnology-based approaches already reach the required LOD for miRNA analysis even in samples with very low miRNA content and may produce sufficient readout signal even without enzymatic amplification. However, many studies in this field stop at the proof-of-principle level, only use fully synthetic or spiked-in samples for technology assessment, do not use stringent controls for selectivity, do not assess sample quality and estimate LOD without considering internationally recognized and recommended procedures. Nanotechnology may give a substantial contribution to cancer diagnosis through quantification of miRNA expression levels, only if 'nanotechnologists' will critically consider all aspects of method development in close collaboration with biologists, clinicians and statisticians. Yet, this field is currently flourishing and there are plenty of opportunities to develop truly innovative approaches for miRNA detection.

Finally, we anticipate that strategies employing nanoparticulate materials in solution may likely become actual qRT-PCR competitors, similar to what is happening with bead-based technologies, for example, xMAP from Luminex, the Firefly from Firefly BioWorks, or the nCounter system from NanoString Technologies. On the other hand, surface-based strategies, with or without the concurrent use of NPs, are better suited for multiplexing analysis in form of arrays. At present, there are no nanotechnology-based strategies allowing the discovery of new miRNAs and for this purpose NGS remains unsurpassed.

Acknowledgements

The author thanks C Frauer for insightful comments and for proofreading the manuscript.

Financial & competing interests disclosure

The author has no relevant affiliations or financial involvement with any organization or entity with a financial interest in or financial conflict with the subject matter or materials discussed in the manuscript. This includes employment, consultancies, honoraria, stock ownership or options, expert testimony, grants or patents received or pending, or royalties.

No writing assistance was utilized in the production of this manuscript.

Supplementary data

To view the supplementary data that accompany this paper, please visit the journal website at: www.futuremedicine.com/doi/full/10.2217/bmm-2016-0195

Executive summary

miRNA detection & quantification for cancer diagnosis

- miRNAs, small noncoding RNAs, play a fundamental role as regulators of gene expression. Dysregulated miRNA expression levels are characteristics of cancer.
- Each type of cancer is characterized by altered expression of a panel of miRNA members. Identification of the minimal, representative miRNA panel is a prerequisite for secure diagnosis.

Challenges faced by miRNA quantification methods

- The miRNA detection method need to be selective, sensitive and has a low limit of detection especially when applied to samples derived from body fluids. They should also have potential for multiplexing.

Nanotechnology-based methods for miRNA quantification

- Can be divided into three main groups: methods in solution involving nanoparticles (NPs), methods based on nanostructured surfaces and methods based on the combination of nanoparticulate materials with solid supports.
- Silver nanoclusters, gold nanoparticles (AuNPs), quantum dots (QDs) and carbonaceous NPs are mainly exploited in quantification strategies based on optical detection. AuNPs can also be used simply as multivalent material for amplification strategies based on mass. Magnetic NPs can work as transducing elements for strategies exploiting nuclear magnetic resonance measurements (ΔT_2).
- miRNA quantification strategies based on nanostructured solid supports are currently mainly used in conjunction with optical readout.
- Carbonaceous NPs and AuNPs deposited on solid supports are used in optical as well as electrochemical quantification strategies.

Future perspective

- Nanotechnology-based approaches already reach the required limit of detection for miRNA analysis even in samples with very low miRNA content.
- Sufficient readout signal may be generated even without enzymatic amplification.
- Newly developed methods are not always tested on real biological samples under relevant conditions.
- There is still an urgent need for standardization in every aspect of miRNA quantification.

References

Papers of special note have been highlighted as:
• of interest; •• of considerable interest

1 Hammond SM. An overview of microRNAs. *Adv. Drug Deliv. Rev.* 87, 3–14 (2015).

2 Huntzinger E, Izaurralde E. Gene silencing by microRNAs: contributions of translational repression and mRNA decay. *Nat. Rev. Genet.* 12(2), 99–110 (2011).

3 Nicoloso MS, Spizzo R, Shimizu M, Rossi S, Calin GA. MicroRNAs – the micro steering wheel of tumour metastases. *Nat. Rev. Cancer* 9(4), 293–302 (2009).

4 Filipowicz W, Bhattacharyya SN, Sonenberg N. Mechanisms of post-transcriptional regulation by microRNAs: are the answers in sight? *Nat. Rev. Genet.* 9(2), 102–114 (2008).

5 Friedman RC, Farh KK-H, Burge CB, Bartel DP. Most mammalian mRNAs are conserved targets of microRNAs. *Genome Res.* 19(1), 92–105 (2009).

6 Pichler M, Calin GA. MicroRNAs in cancer: from developmental genes in worms to their clinical application in patients. *Br. J. Cancer* 113(4), 569–573 (2015).

7 Di Leva G, Garofalo M, Croce CM. MicroRNAs in cancer. *Annu. Rev. Pathol.: Mech. Dis.* 9(1), 287–314 (2014).

8 Di Leva G, Croce CM. miRNA profiling of cancer. *Curr. Opin. Genet. Dev.* 23(1), 3–11 (2013).

9 Farazi TA, Spitzer JI, Morozov P, Tuschl T. miRNAs in human cancer. *J. Pathol.* 223(2), 102–115 (2011).

10 Mitchell PS, Parkin RK, Kroh EM *et al.* Circulating microRNAs as stable blood-based markers for cancer detection. *Proc. Natl Acad. Sci. USA* 105(30), 10513–10518 (2008).

11 Chen X, Ba Y, Ma L *et al.* Characterization of microRNAs in serum: a novel class of biomarkers for diagnosis of cancer and other diseases. *Cell Res.* 18(10), 997–1006 (2008).

12 Larrea E, Sole C, Manterola L *et al.* New concepts in cancer biomarkers: circulating miRNAs in liquid biopsies. *Int. J. Mol. Sci.* 17(5), pii: E627 (2016).

13 Khoury S, Tran N. Circulating microRNAs: potential biomarkers for common malignancies. *Biomarkers Med.* 9(2), 131–151 (2015).

14 Tiberio P, Callari M, Angeloni V, Daidone MG, Appierto V. Challenges in using circulating miRNAs as cancer biomarkers. *BioMed Res. Int.* 2015, 731479 (2015).

15 He Y, Lin J, Kong D *et al.* Current state of circulating microRNAs as cancer biomarkers. *Clin. Chem.* 61(9), 1138–1155 (2015).

16 Weber JA, Baxter DH, Zhang S *et al.* The microRNA spectrum in 12 body fluids. *Clin. Chem.* 56(11), 1733–1741 (2010).

17 Witwer KW. Circulating microRNA biomarker studies: pitfalls and potential solutions. *Clin. Chem.* 61(1), 56 (2014).

18 Redshaw N, Wilkes T, Whale A, Cowen S, Huggett J, Foy CA. A comparison of miRNA isolation and RT-qPCR technologies and their effects on quantification accuracy and repeatability. *Biotechniques* 54(3), 155–164 (2013).

19 McDonald JS, Milosevic D, Reddi HV, Grebe SK, Algeciras-Schimnich A. Analysis of circulating microRNA: preanalytical and analytical challenges. *Clin. Chem.* 57(6), 833–840 (2011).

20 El-Khoury V, Pierson S, Kaoma T, Bernardin F, Berchem G. Assessing cellular and circulating miRNA recovery: the impact of the RNA isolation method and the quantity of input material. *Sci. Rep.* 6, 19529 (2016).

21 Schwarzenbach H, da Silva AM, Calin G, Pantel K. Data normalization strategies for microRNA quantification. *Clin. Chem.* 61(11), 1333 (2015).

22 Meyer S, Pfaffl M, Ulbrich S. Normalization strategies for microRNA profiling experiments: a 'normal' way to a hidden layer of complexity? *Biotechnol. Lett* 32(12), 1777–1788 (2010).

23 Knutsen E, Fiskaa T, Ursvik A *et al.* Performance comparison of digital microRNA profiling technologies applied on human breast cancer cell lines. *PLoS ONE* 8(10), e75813 (2013).

24 Kelly H, Downing T, Tuite NL *et al.* Cross platform standardisation of an experimental pipeline for use in the identification of dysregulated human circulating miRNAs. *PLoS ONE* 10(9), e0137389 (2015).

25 Git A, Dvinge H, Salmon-Divon M *et al.* Systematic comparison of microarray profiling, real-time PCR, and next-generation sequencing technologies for measuring differential microRNA expression. *RNA* 16(5), 991–1006 (2010).

26 Chen C, Ridzon DA, Broomer AJ *et al.* Real-time quantification of microRNAs by stem–loop RT–PCR. *Nucleic Acids Res.* 33(20), e179 (2005).

27 Neilson JR, Zheng GXY, Burge CB, Sharp PA. Dynamic regulation of miRNA expression in ordered stages of cellular development. *Genes Dev.* 21(5), 578–589 (2007).

28 Bissels U, Wild S, Tomiuk S *et al.* Absolute quantification of microRNAs by using a universal reference. *RNA* 15(12), 2375–2384 (2009).

29 Liang Y, Ridzon D, Wong L, Chen C. Characterization of microRNA expression profiles in normal human tissues. *BMC Genomics* 8(1), 1–20 (2007).

30 Moret I, Sánchez-Izquierdo D, Iborra M *et al.* Assessing an improved protocol for plasma microRNA extraction. *PLoS ONE* 8(12), e82753 (2013).

31 Mangolini A, Ferracin M, Zanzi MV *et al.* Diagnostic and prognostic microRNAs in the serum of breast cancer patients measured by droplet digital PCR. *Biomark. Res.* 3(1), 1–9 (2015).

32 Flowers E, Froelicher ES, Aouizerat BE. Measurement of microRNA: a regulator of gene expression. *Biol. Res. Nurs.* 15(2), 167–178 (2013).

33 Pritchard CC, Cheng HH, Tewari M. MicroRNA profiling: approaches and considerations. *Nat. Rev. Genet.* 13(5), 358–369 (2012).

34 Li D, Wang Y, Lau C, Lu J. xMAP array microspheres based stem–loop structured probes as conformational switches for multiplexing detection of miRNAs. *Anal. Chem.* 86(20), 10148–10156 (2014).

35 Chapin SC, Appleyard DC, Pregibon DC, Doyle PS. Rapid microRNA profiling on encoded gel microparticles. *Angew. Chem. Int. Ed.* 50(10), 2289–2293 (2011).

36 Geiss GK, Bumgarner RE, Birditt B *et al.* Direct multiplexed measurement of gene expression with color-coded probe pairs. *Nat. Biotechnol.* 26(3), 317–325 (2008).

37 Chatterjee A, Leichter AL, Fan V *et al.* A cross comparison of technologies for the detection of microRNAs in clinical FFPE samples of hepatoblastoma patients. *Sci. Rep.* 5, 10438 (2015).

38 Mestdagh P, Hartmann N, Baeriswyl L *et al.* Evaluation of quantitative miRNA expression platforms in the microRNA quality control (miRQC) study. *Nat. Methods* 11(8), 809–815 (2014).

39 Kolbert CP, Feddersen RM, Rakhshan F *et al.* Multi-platform analysis of microRNA expression measurements in RNA from fresh frozen and FFPE tissues. *PLoS ONE* 8(1), e52517 (2013).

40 Hunt EA, Broyles D, Head T, Deo SK. MicroRNA detection: current technology and research strategies. *Annu. Rev. Anal. Chem.* 8(1), 217–237 (2015).

41 Tian T, Wang J, Zhou X. A review: microRNA detection methods. *Org. Biomol. Chem.* 13(8), 2226–2238 (2015).

42 Degliangeli F, Pompa PP, Fiammengo R. Nanotechnology-based strategies for the detection and quantification of microRNA. *Chem. Eur. J.* 20(31), 9476–9492 (2014).

•• **Recent, comprehensive review on miRNA quantification using nanotechnology-based strategies.**

43 Syedmoradi L, Daneshpour M, Alvandipour M, Gomez FA, Hajghassem H, Omidfar K. Point of care testing: the impact of nanotechnology. *Biosens. Bioelectron.* 87, 373–387 (2017).

44 Petty JT, Zheng J, Hud NV, Dickson RM. DNA-templated Ag nanocluster formation. *J. Am. Chem. Soc.* 126(16), 5207–5212 (2004).

45 Diez I, Ras RHA. Fluorescent silver nanoclusters. *Nanoscale* 3(5), 1963–1970 (2011).

46 Yang SW, Vosch T. Rapid detection of microRNA by a silver nanocluster DNA probe. *Anal. Chem.* 83(18), 6935–6939 (2011).

47 Shah P, Choi SW, Kim H-j *et al.* Locking-to-unlocking system is an efficient strategy to design DNA/silver nanoclusters (AgNCs) probe for human miRNAs. *Nucleic Acids Res.* 44(6), e57 (2016).

48 Shah P, Choi SW, Kim H-j *et al.* DNA/RNA chimera templates improve the emission intensity and target the accessibility of silver nanocluster-based sensors for human microRNA detection. *Analyst* 140(10), 3422–3430 (2015).

49 Shah P, Thulstrup PW, Cho SK *et al.* In-solution multiplex miRNA detection using DNA-templated silver nanocluster probes. *Analyst* 139(9), 2158–2166 (2014).

50 CLSI/NCCLS. *Protocols for Determination of Limit of Detection and Limits of Quantitation; Approved Guideline.* CLSI Document EP17-A. Clinical and Laboratory Standards Institute, Wayne, PA, USA (2004).

51 International Organization for Standardization. Methodology in the linear and non-linear calibration case. In: *Capability Of Detection (Part 5.).* International Organization for Standardization, Geneva, Switzerland (2008).

52 CLSI. Evaluation of Detection Capability For Clinical Laboratory Measurement Procedures; Approved Guideline (2nd Edition). *CLSI Document EP17-A2.* Clinical and Laboratory Standards Institute, Wayne, PA, USA (2012).

53 Needleman SB, Romberg RW. Limits of linearity and detection for some drugs of abuse. *J. Anal. Toxicol.* 14(1), 34–38 (1990).

54 Huang S, Wang T, Yang M. The evaluation of statistical methods for estimating the lower limit of detection. *Assay Drug Dev. Technol.* 11(1), 35–43 (2013).

55 Zhang M, Liu Y-Q, Yu C-Y, Yin B-C, Ye B-C. Multiplexed detection of microRNAs by tuning DNA-scaffolded silver nanoclusters. *Analyst* 138(17), 4812–4817 (2013).

56 Liu Y-Q, Zhang M, Yin B-C, Ye B-C. Attomolar ultrasensitive microRNA detection by DNA-scaffolded silver-nanocluster probe based on isothermal amplification. *Anal. Chem.* 84(12), 5165–5169 (2012).

57 Dong H, Hao K, Tian Y *et al.* Label-free and ultrasensitive microRNA detection based on novel molecular beacon binding readout and target recycling amplification. *Biosens. Bioelectron.* 53(0), 377–383 (2014).

58 Zhang J, Li C, Zhi X *et al.* Hairpin DNA-templated silver nanoclusters as novel beacons in strand displacement amplification for microRNA detection. *Anal. Chem.* 88(2), 1294–1302 (2016).

59 Li R-D, Wang Q, Yin B-C, Ye B-C. Enzyme-free detection of sequence-specific microRNAs based on nanoparticle-assisted signal amplification strategy. *Biosens. Bioelectron.* 77, 995–1000 (2016).

60 Degliangeli F, Kshirsagar P, Brunetti V, Pompa PP, Fiammengo R. Absolute and direct microRNA quantification using DNA–gold nanoparticle probes. *J. Am. Chem. Soc.* 136(6), 2264–2267 (2014).

• **Single step, solution-based assay allowing quantification of as little as 100 copies of miRNAs per cell in samples of extracted total RNA.**

61 He X, Zeng T, Li Z, Wang G, Ma N. Catalytic molecular imaging of microRNA in living cells by DNA-programmed nanoparticle disassembly. *Angew. Chem. Int. Ed.* 55(9), 3073–3076 (2016).

62 Wang Q, Li R-D, Yin B-C, Ye B-C. Colorimetric detection of sequence-specific microRNA based on duplex-specific nuclease-assisted nanoparticle amplification. *Analyst* 140(18), 6306–6312 (2015).

63 Lee H, Park J-E, Nam J-M. Bio-barcode gel assay for microRNA. *Nat. Commun.* 5, 3367 (2014).

64 Chen S, Chu LT, Yeung PP *et al.* Enzyme-free amplification by nano sticky balls for visual detection of ssDNA/RNA oligonucleotides. *ACS Appl. Mater. Interfaces* 7(41), 22821–22830 (2015).

65 Zhou X, Cao P, Zhu Y, Lu W, Gu N, Mao C. Phage-mediated counting by the naked eye of miRNA molecules at attomolar concentrations in a Petri dish. *Nat. Mater.* 14(10), 1058–1064 (2015).

66 Jou AF-j, Lu C-H, Ou Y-C *et al.* Diagnosing the miR-141 prostate cancer biomarker using nucleic acid-functionalized CdSe/ZnS QDs and telomerase. *Chem. Sci.* 6(1), 659–665 (2015).

67 Pang Y, Wang C, Wang J, Sun Z, Xiao R, Wang S. Fe3O4@Ag magnetic nanoparticles for microRNA capture and duplex-specific nuclease signal amplification based SERS detection in cancer cells. *Biosens. Bioelectron.* 79, 574–580 (2016).

• **Assay with excellent LOD, large dynamic range and simple implementation.**

68 Lu C-H, Yang H-H, Zhu C-L, Chen X, Chen G-N. A graphene platform for sensing biomolecules. *Angew. Chem. Int. Ed.* 48(26), 4785–4787 (2009).

69 Liu B, Sun Z, Zhang X, Liu J. Mechanisms of DNA sensing on graphene oxide. *Anal. Chem.* 85(16), 7987–7993 (2013).

70 Robertson NM, Salih Hizir M, Balcioglu M *et al.* Discriminating a single nucleotide difference for enhanced miRNA detection using tunable graphene and oligonucleotide nanodevices. *Langmuir* 31(36), 9943–9952 (2015).

71 Bi S, Chen M, Jia X, Dong Y. A hot-spot-active magnetic graphene oxide substrate for microRNA detection based on cascaded chemiluminescence resonance energy transfer. *Nanoscale* 7(8), 3745–3753 (2015).

72 Wu Y, Han J, Xue P, Xu R, Kang Y. Nano metal-organic framework (NMOF)-based strategies for multiplexed microRNA detection in solution and living cancer cells. *Nanoscale* 7(5), 1753–1759 (2015).

73 Wang Q, Yin B-C, Ye B-C. A novel polydopamine-based chemiluminescence resonance energy transfer method for microRNA detection coupling duplex-specific nuclease-aided target recycling strategy. *Biosens. Bioelectron.* 80, 366–372 (2016).

74 Lu W, Chen Y, Liu Z *et al.* Quantitative detection of microRNA in one step via next generation magnetic relaxation switch sensing. *ACS Nano* 10(7), 6685–6692 (2016).

• **Assay with nuclear magnetic resonance detection. Quantification of miR-21 in total RNA from excised liver tumors and surrounding tissues.**

75 Yin F, Liu H, Li Q, Gao X, Yin Y, Liu D. Trace microRNA quantification by means of plasmon-enhanced hybridization chain reaction. *Anal. Chem.* 88(9), 4600–4604 (2016).

76 Liu Q, Shin Y, Kee JS *et al.* Mach–Zehnder interferometer (MZI) point-of-care system for rapid multiplexed detection of microRNAs in human urine specimens. *Biosens. Bioelectron.* 71, 365–372 (2015).

77 Huertas CS, Fariña D, Lechuga LM. Direct and Label-free quantification of micro-RNA-181a at attomolar level in complex media using a nanophotonic biosensor. *ACS Sensors* 1(6), 748–756 (2016).

•• **Good intrinsic multiplexing capability. Quantification of miR-181a directly in urine samples.**

78 Wang Q, Li Q, Yang X *et al.* Graphene oxide–gold nanoparticles hybrids-based surface plasmon resonance for sensitive detection of microRNA. *Biosens. Bioelectron.* 77, 1001–1007 (2016).

79 Cai B, Huang L, Zhang H, Sun Z, Zhang Z, Zhang G-J. Gold nanoparticles-decorated graphene field-effect transistor biosensor for femtomolar microRNA detection. *Biosens. Bioelectron.* 74, 329–334 (2015).

80 Cheng F-F, He T-T, Miao H-T, Shi J-J, Jiang L-P, Zhu J-J. Electron transfer mediated electrochemical biosensor for microRNAs detection based on metal ion functionalized titanium phosphate nanospheres at attomole level. *ACS Appl. Mater. Interfaces* 7(4), 2979–2985 (2015).

• **Multistep assay with electrochemical readout suitable for miR-21 quantification in serum samples. Record low LOD (4 ymol).**

81 Azimzadeh M, Rahaie M, Nasirizadeh N, Ashtari K, Naderi-Manesh H. An electrochemical nanobiosensor for plasma miRNA-155, based on graphene oxide and gold nanorod, for early detection of breast cancer. *Biosens. Bioelectron.* 77, 99–106 (2016).

82 Cao H, Liu S, Tu W, Bao J, Dai Z. A carbon nanotube/quantum dot based photoelectrochemical biosensing platform for the direct detection of microRNAs. *Chem. Commun.* 50(87), 13315–13318 (2014).

83 Yin H, Zhou Y, Li B *et al.* Photoelectrochemical immunosensor for microRNA detection based on gold nanoparticles-functionalized g-C3N4 and anti-DNA:RNA antibody. *Sensors Actuators B Chem.* 222, 1119–1126 (2016).

84 Wang Y, MacLachlan E, Nguyen BK, Fu G, Peng C, Chen JIL. Direct detection of microRNA based on plasmon hybridization of nanoparticle dimers. *Analyst* 140(4), 1140–1148 (2015).

85 Roy S, Soh JH, Ying JY. A microarray platform for detecting disease-specific circulating miRNA in human serum. *Biosens. Bioelectron.* 75, 238–246 (2016).

86 Joshi GK, Deitz-McElyea S, Johnson M, Mali S, Korc M, Sardar R. Highly specific plasmonic biosensors for ultrasensitive microRNA detection in plasma from pancreatic cancer patients. *Nano Lett.* 14(12), 6955–6963 (2014).

87 Joshi GK, Deitz-McElyea S, Liyanage T *et al.* Label-free nanoplasmonic-based short noncoding RNA sensing at attomolar concentrations allows for quantitative and highly specific assay of microRNA-10b in biological fluids and circulating exosomes. *ACS Nano* 9(11), 11075–11089 (2015).

• **Quantification of plasma and exosomal miR-10b.**

88 Liu S, Su W, Li Z, Ding X. Electrochemical detection of lung cancer specific microRNAs using 3D DNA origami nanostructures. *Biosens. Bioelectron.* 71, 57–61 (2015).

89 Miao P, Tang Y, Wang B *et al.* Nuclease assisted target recycling and spherical nucleic acids gold nanoparticles recruitment for ultrasensitive detection of microRNA. *Electrochim. Acta* 190, 396–401 (2016).

90 Miao X, Wang W, Kang T *et al.* Ultrasensitive electrochemical detection of miRNA-21 by using an iridium(III) complex as catalyst. *Biosens. Bioelectron.* 86, 454–458 (2016).